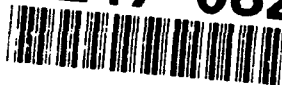


AD-A247 082



OFFICE OF NAVAL RESEARCH

Contract N00014-82K-0612

Task No. NR 627-838

TECHNICAL REPORT NO. 65

Microhole Array Electrodes Based on  
Microporous Alumina Membranes

by

Charles J. Brumlik, Charles R. Martin and Koichi Tokuda

Department of Chemistry  
Colorado State University  
Ft. Collins, CO 80523

Prepared for publication

in

Analytical Chemistry

February 25, 1992

Reproduction in whole or part is permitted for  
any purpose of the United States Government

\*This document has been approved for public release  
and sale; its distribution is unlimited

\*This statement would also appear in Item 10 of Document  
Control Data - DD Form 1473. Copies of form  
Available from cognizant contract administrator

DTIC  
ELECTE  
MAR 5 1992  
S C D

92 3 03 057

92-05584



## REPORT DOCUMENTATION PAGE

Form Approved  
OMB No. 0704-0188

1a. REPORT SECURITY CLASSIFICATION UNCLASSIFIED			1b. RESTRICTIVE MARKINGS		
2a. SECURITY CLASSIFICATION AUTHORITY			3. DISTRIBUTION / AVAILABILITY OF REPORT APPROVED FOR PUBLIC DISTRIBUTION, DISTRIBUTION UNLIMITED.		
2b. DECLASSIFICATION / DOWNGRADING SCHEDULE					
4. PERFORMING ORGANIZATION REPORT NUMBER(S)  ONR TECHNICAL REPORT #65			5. MONITORING ORGANIZATION REPORT NUMBER(S)		
6a. NAME OF PERFORMING ORGANIZATION Dr. Charles R. Martin Department of Chemistry		6b. OFFICE SYMBOL (If applicable)	7a. NAME OF MONITORING ORGANIZATION  Office of Naval Research		
6c. ADDRESS (City, State, and ZIP Code) Colorado State University Ft. Collins, CO 80523			7b. ADDRESS (City, State, and ZIP Code) 800 North Quincy Street Arlington, VA 22217		
8a. NAME OF FUNDING / SPONSORING ORGANIZATION Office of Naval Research		8b. OFFICE SYMBOL (If applicable)	9. PROCUREMENT INSTRUMENT IDENTIFICATION NUMBER  Contract # N00014-82K-0612		
8c. ADDRESS (City, State, and ZIP Code) 800 North Quincy Street Arlington, VA 22217			10. SOURCE OF FUNDING NUMBERS		
			PROGRAM ELEMENT NO.	PROJECT NO.	TASK NO.
11. TITLE (Include Security Classification) Microhole Array Electrodes Based on Microporous Alumina Membranes					
12. PERSONAL AUTHOR(S) Charles J. Brumlik, Charles R. Martin and Koichi Tokuda					
13a. TYPE OF REPORT Technical		13b. TIME COVERED FROM _____ TO _____		14. DATE OF REPORT (Year, Month, Day) 1992, 2, 25	
15. PAGE COUNT					
16. SUPPLEMENTARY NOTATION					
17. COSATI CODES			18. SUBJECT TERMS (Continue on reverse if necessary and identify by block number)  Ultramicroelectrodes, microhole electrodes, membrane electrochemistry		
FIELD	GROUP	SUB-GROUP			
19. ABSTRACT (Continue on reverse if necessary and identify by block number)  A procedure for preparing microhole array electrodes is described. These electrodes are based on a microporous alumina filtration membrane. This membrane (Anopore) contains linear 200 nm diameter pores. These pores define the holes in the microhole array. The microelectrodes at the bottoms of the holes are formed by simply coating the back of the membrane with gold. This procedure yields an electrode with a high density of uniform microholes. Furthermore, this microhole array electrode combines very deep microholes with the smallest microhole diameters (200 nm) to be reported in the literature to date. Cyclic voltammetry was used to characterize these electrodes.					
20. DISTRIBUTION / AVAILABILITY OF ABSTRACT <input checked="" type="checkbox"/> UNCLASSIFIED/UNLIMITED <input type="checkbox"/> SAME AS RPT. <input type="checkbox"/> DTIC USERS			21. ABSTRACT SECURITY CLASSIFICATION UNCLASSIFIED		
22a. NAME OF RESPONSIBLE INDIVIDUAL Dr. Robert Nowak			22b. TELEPHONE (Include Area Code) (202) 696-4410		22c. OFFICE SYMBOL

**MICROHOLE ARRAY ELECTRODES BASED ON  
MICROPOROUS ALUMINA MEMBRANES**

Charles J. Brumlik and Charles R. Martin\*  
Department of Chemistry  
Colorado State University  
Fort Collins, CO 80523

Koichi Tokuda  
Department of Electronic Chemistry  
Tokyo Institute of Technology Nagatsuta  
Midori-ku, Yokohama 227, Japan



\*To whom correspondence should be addressed.

<b>Accession For</b>	
NTIS GRA&I	<input checked="" type="checkbox"/>
DTIC TAB	<input type="checkbox"/>
Unannounced	<input type="checkbox"/>
Justification	
By	
Distribution/	
Availability Codes	
Dist	Avail and/or Special
A-1	

### Abstract

A procedure for preparing microhole array electrodes is described. These electrodes are based on a microporous alumina filtration membrane. This membrane (Anopore) contains linear 200 nm diameter pores. These pores define the holes in the microhole array. The microelectrodes at the bottoms of the holes are formed by simply coating the back of the membrane with gold. This procedure yields an electrode with a high density of uniform microholes. Furthermore, this microhole array electrode combines very deep microholes with the smallest microhole diameters (200 nm) to be reported in the literature to date. Cyclic voltammetry was used to characterize these electrodes.

## BRIEF

Microhole array electrodes with microelectrode diameters of 200 nm and recesses of 60  $\mu\text{m}$  were prepared and characterized.

## INTRODUCTION

Majda et al. developed and investigated modified electrodes based on microporous alumina membranes (1-8). The membranes had cylindrical pores of equivalent diameter and were prepared via a derivative of a classical electrochemical method (9-11). Majda et al. attached various electroactive molecules to the pore walls and investigated rates of lateral electron transfer in these membranes. More recently, related electrochemical devices - "microhole" and "microhole array" electrodes - were developed and investigated by Bond et al. (12) and Shimizu et al. (13-17). These are related devices because the electrode elements are recessed within pores. These devices are used as electrochemical detectors for electroactive analyte molecules in a contacting solution phase (14,17). The key advantage of such detectors is that the electrochemical signal is insensitive to convection or flow in the contacting solution phase, because the electrode element is recessed (15).

Microhole array electrodes have previously been prepared by potting carbon fibers in epoxy and then electropolishing the carbon so that the ends of the fibers are recessed within the epoxy (13-17). The increasing interest in microhole array electrodes (e.g. such electrodes are now commercially available (18)) prompted us to ask whether microporous alumina membranes might be useful for preparing arrays of microhole electrodes. The advantage of this approach is that because the thickness, pore density, and pore diameter of the microporous alumina membrane can be controlled by varying the anodization procedure (9-11), microhole array electrodes with any desired characteristics could be prepared. In this technical note we demonstrate that microporous alumina membranes can be used to prepare microhole array electrodes. We also show that the faradaic response characteristics of these electrodes are in agreement with predictions of the relevant transport theories (12,15,19,20).

## EXPERIMENTAL

Electrode Preparation. Commercially-available Anopore™ alumina filters were obtained from Anotec Separations; these membranes are 60  $\mu\text{m}$  thick, contain 200 nm-diameter pores, and are ca. 65 % porous (21-24). An RF magnetron Ar plasma deposition system (Hummer VI, Anatech) was used to coat one face of the Anopore membrane with a thin (20 nm) gold film (23). This film served as a cathode for electroplating a thick (5  $\mu\text{m}$ ) Au film onto the membrane surface. The plating solution was Orotemp 24 (Technics) (22,23). A one-compartment cell consisting of the Au/Anopore working electrode and a platinized niobium mesh counter electrode was used. Au was deposited galvanostatically (0.8-1.2  $\text{mA}/\text{cm}^2$ ) to a total charge of 5  $\text{C}/\text{cm}^2$ . We prefer this electrochemical method (22,23) to vacuum evaporation (1-8); evaporated films often peeled away from the membrane surface. The electrodeposited films adhere strongly because gold deposits a short distance (1  $\mu\text{m}$ ) into the pores. Hence, an array of Au microfibers (21-23) "anchors" the Au film to the membrane.

After electroplating, the Au/Anopore membranes were washed with water and dried in air. A 3/8" diameter circle was then punched from the membrane using a shim stock punch and die set. This disk was attached with silver-epoxy (410E, Epo-Tek) onto an end of a 3/8" diameter stainless steel rod which served as a current collector. The edges and sides of the electrodes were insulated with Torr Seal epoxy. Ideally (see below), the disk-shaped surfaces of the Au microfibers at the bottom of each pore define the active working electrode area. The depth of the microholes is then just the thickness of the membrane (60  $\mu\text{m}$ ) minus the length of the Au fiber (21-23) (1  $\mu\text{m}$ ).

Electrochemical Measurements. Electrochemical measurements were carried out in a single-compartment glass cell containing the microhole array working electrode, the platinized

niobium mesh counter electrode, and an aqueous Ag/AgCl reference electrode (BAS) or a non-aqueous Ag/AgNO<sub>3</sub> reference electrode (0.1M AgNO<sub>3</sub> in DMSO). Both double layer charging and faradaic currents were investigated (25-28). Faradaic currents at the array electrodes were investigated in both aqueous and nonaqueous solutions. The aqueous solutions were 4.74 mM in K<sub>3</sub>Fe(CN)<sub>6</sub> and 1 M in KCl. The nonaqueous solutions were 1.60 mM in ferrocene and 0.2 M in LiClO<sub>4</sub> (in DMSO). The microhole array electrodes were soaked in the desired solution for at least 30 minutes prior to the electrochemical measurements to insure maximal wetting of the microholes.

Charging currents were used to determine the electroactive surface areas of the microhole electrodes (25-28). Both aqueous and nonaqueous solutions were investigated. The aqueous solution was 1 M in KCl and 0.2 (v/v) % in S-1 (Technics) surfactant; the surfactant was added to improve wetting of the pores. The nonaqueous electrolyte solution was 0.2 M in LiClO<sub>4</sub> (in DMSO). Electroactive surface areas were obtained by comparing the double layer charging current at the array to analogous currents at an Au disk macro-electrode of known area (25-28). We have used these methods extensively in our investigations of ultramicrodisk electrodes (25-28). Typical voltammograms are shown in Figure 1. To avoid unwanted residual faradaic currents (25) the charging currents were measured at 0 V. The analogous background voltammogram at the array electrode (Figure 1) shows a pronounced slope, caused by the resistance of the solution within the pores of the membrane. As in our previous studies, we circumvented this problem by measuring both the anodic and cathodic current at a particular potential (in this case 0 V) and averaging the absolute magnitudes of these currents to obtain the double layer charging current.



Enhancing Performance in Aqueous Solution. Charging currents in aqueous solution increased with the duration of exposure of the electrode to the solution. As was the case with our previous electrodes (25-28), this problem is caused by "creeping" of the solution between the Au microfibers and the alumina membrane. We have attempted to solve this problem by improving the adhesion between the Au and the alumina membrane. This was accomplished by treating the membrane with 2-cyanoethyltriethoxysilane (Petrarch) prior to deposition of the Au film (23). This silane was chosen because our prior investigations have shown that the cyano group interacts strongly with gold (23). Silanization was accomplished by sonicating the membrane in a 0.5 (w/w) % solution of the silane in anhydrous hexadecane for 30 seconds. The membrane was then dried at 100° C overnight.

## **RESULTS AND DISCUSSION**

Electroactive Surface Areas. Ideally, the electroactive surface area is simply the product of the known geometric area of the array electrode and the known porosity of the membrane (25-28); however, if solvent can creep between the pore wall and the Au fiber, the measured electroactive surface area will be larger than this ideal value (25-28). This excess surface area is undesirable because it increases the background charging current; this is a common problem with microelectrodes (27,29). Typical electroactive surface area data for three microhole array electrodes are presented in Table I. The data are expressed as the ratio of the measured area to the ideal area. When DMSO is the solvent, the measured area for the array is essentially identical to the ideal area, even after 5 hours of continuous use in the DMSO/supporting electrolyte solution (Table I).

In contrast, when water is the solvent, the electroactive surface area is initially somewhat smaller than the ideal area (because a fraction of the pores are not wetted) but becomes much larger than the ideal area after 5 hours of use. This indicates that water is creeping between the Au fibers and the pore wall (25,28). The severity of this water-creeping problem can be mitigated by treating the surface of the Anopore membrane with the cyano-containing silane. As indicated in Table I, the electroactive surface area for the silane-treated array increased by only a factor of 2 after 5 hours of continuous use in the aqueous electrolyte solution. This is a substantial improvement relative to the array prepared from the untreated Anopore membrane (Table I). Furthermore, the cyano-derivatized membrane is more easily wetted by water than the virgin membrane because the derivatized membrane initially shows the ideal electroactive area (Table I). Thus, derivatization of the membrane is an important component of the electrode fabrication process.

Faradaic Response. As discussed in detail by others (12,15,19,20,30) the shape of the voltammogram obtained at a microhole electrode is dependant on the scan rate and the depth of the microhole. In a high scan rate experiment, the diffusion layers at the recessed electrodes are confined within the membrane and do not propagate into the bulk solution phase. Thus, a conventional peak-shaped, semi-infinite linear diffusion voltammogram is obtained. The scan rate region over which this semi-infinite diffusion situation prevails depends on the depth of the microhole (see below). The voltammograms shown in Figure 2A illustrate this limiting case. As indicated earlier, one of the advantages of microhole electrodes is independence of the voltammogram from convection in the solution (15). This

effect is also illustrated in Figure 2A; note that voltammograms obtained from a quiescent and a vigorously stirred solution are essentially identical.

At low scan rates, the diffusion layers created at the recessed Au electrodes will become thicker than the depth of the microhole (12,15,19,20,30). The shape of the voltammogram then depends on whether the solution is stirred or unstirred. If the solution is unstirred, the diffusion layers propagate into the bulk solution and overlap to form a diffusion field which extends linearly from the surface of the Anopore membrane; this "total overlap" (26) limiting case is assured because of the high pore density of this membrane. If the solution is stirred, the diffusion layers cannot propagate into the bulk solution. Thus the diffusion layer becomes confined to the depth of the microhole plus the thickness of the unstirred nernst layer at the membrane surface (15). In this case, a finite diffusion (i.e. plateau-shaped) voltammogram will be obtained (15). The transition from the semi-infinite to the finite diffusion cases is illustrated in Figure 2B.

This transition can be shown more quantitatively by plotting the peak or plateau current vs. the square root of scan rate (Figure 3). As indicated in Figure 3, this transition occurs at ca.  $10 \text{ mV s}^{-1}$ . A simple analysis shows that this "transition scan rate" ( $\nu_t$ ) is reasonable, given the depth of the microholes investigated here;  $\nu_t$  can be converted to a corresponding transition time ( $\tau$ ) via

$$\tau = RT/(F\nu_t) \quad (1)$$

A  $\tau$  of 2.57 s is obtained. The average distance (d) that a diffusion layer will move in this 2.57 s time interval is given by

$$d = (2D\tau)^{1/2} \quad (2)$$

where  $D$  is the diffusion coefficient. Equation 2 predicts that  $\text{Fe(CN)}_6^{4-}$  ( $D = 7.6 \times 10^{-6} \text{ cm}^2 \text{ s}^{-1}$  (31)) will diffuse, on average,  $62 \mu\text{m}$  in  $2.57 \text{ s}$ . This is in good agreement with the  $59 \mu\text{m}$  depth of the microholes in our electrodes. That the calculated thickness is somewhat larger than the depth of the microhole is to be expected because, as indicated above, the diffusion layer must traverse both the depth of the microhole and the thickness of the unstirred Nernst layer at the electrode surface (15).

## CONCLUSIONS

The data in Figure 2 and 3, as well as the analysis presented above, show that the faradaic response characteristics of these microhole array electrodes are in agreement with the predictions of the relevant electrochemical theory (12,15,19). We have shown, however, that care must be taken to seal the electrode/membrane interface to prevent spuriously high background currents. These microhole array electrodes combine very deep microholes with the smallest microhole diameters ( $200 \text{ nm}$ ) to be reported in the literature to date.

## Acknowledgements

This work was supported by the Office of Naval Research.

## References

- (1) Miller, C. J.; Majda, M. *J. Am. Chem. Soc.* **1985**, *107*(5), 1419-1420.
- (2) Miller, C. J.; Majda, M. *J. Electroanal. Chem. Interfacial Electrochem.* **1986**, *207*(1-2), 49-72.
- (3) Miller, C. J.; Majda, M. *J. Am. Chem. Soc.* **1986**, *108*(11), 3118-3120.
- (4) Miller, C. J.; Majda, M. *Anal. Chem.* **1988**, *60*(11), 1168-1176.
- (5) Miller, C. J.; Widrig, C. A.; Charych, D. H.; Majda, M. *J. Phys. Chem.* **1988**, *92*(7), 1928-1936.
- (6) Goss, C. A.; Miller, C. J.; Majda, M. *J. Phys. Chem.* **1988**, *92*(7), 1937-1942.
- (7) Bourdillon, C.; Majda, M. *J. Am. Chem. Soc.* **1990**, *112*(5), 1795-1799.
- (8) Goss, C. A.; Majda, M. *J. Electroanal. Chem. Interfacial Electrochem.* **1991**, *300*(1-2), 377-405.
- (9) Diggle, J. W.; Downie, T. C.; Goulding, C. W. *Chem. Rev.* **1969**, *69*, 365.
- (10) Thompson, G. E.; Wood, G. C. In *Corrosion: Aqueous Processes and Passive Films*, 1st ed.; Scully, J. C., Ed.; Academic Press: London, 1983; p. 205.
- (11) Wood, G. C. In *Oxides and Oxide Films*, 1st ed.; Diggle, J. W., Ed.; Marcel Dekker, Inc.: New York, 1973; Vol. 2, p. 167.
- (12) Bond, A. M.; Luscombe, D.; Oldham, K. B.; Zoski, C. G. *J. Electroanal. Chem. Interfacial Electrochem.* **1988**, *249*, 1.
- (13) Morita, K.; Shimizu, Y. *Anal. Chem.* **1989**, *61*(2), 159-162.
- (14) Shimizu, Y.; Morita, K. *Anal. Chem.* **1990**, *62*(14), 1498-1501.
- (15) Tokuda, K.; Morita, K.; Shimizu, Y. *Anal. Chem.* **1989**, *61*(15), 1763-1768.

- (16) Tokuda, K.; Okamoto, T.; Morita, K.; Shimizu, Y. *Denki Kagaku oyobi Kogyo Butsuri Kagaku* **1990**, *58*, 1217.
- (17) Morita, K.; Shimizu, Y. *Denki Kagaku oyobi Kogyo Butsuri Kagaku* **1990**, *58*(12), 1190-1196.
- (18) Cypress Systems, Inc. Lawrence, Kansas.
- (19) West, A. C.; Newman, J. J. *J. Electrochem. Soc.* **1991**, *138*(6), 1620-1625.
- (20) Diem, C. B.; Newman, B.; Orazem, M. E. *J. Electrochem. Soc.* **1988**, *135*(10), 2524-2530.
- (21) Tierney, M. J.; Martin, C. R. *J. Phys. Chem.* **1989**, *93*, 2878.
- (22) Van Dyke, L. S.; Martin, C. R. *Langmuir* **1990**, *6*, 1118.
- (23) Brumlik, C. J.; Martin, C. R. *J. Am. Chem. Soc.* **1991**, *113*, 3174.
- (24) Liu, C.; Martin, C. R. *Nature* **1991**, *352*, 50.
- (25) Penner, R. M.; Martin, C. R. *Anal. Chem.* **1987**, *59*(21), 2625-2630.
- (26) Cheng, F. I.; Whiteley, L. D.; Martin, C. R. *Anal. Chem.* **1989**, *61*, 762.
- (27) Cheng, I. F.; Martin, C. R. *Anal. Chem.* **1988**, *60*(19), 2163-2165.
- (28) Cheng, I. F.; Schimpf, J. M.; Martin, C. R. *J. Electroanal. Chem. Interfacial Electrochem.* **1990**, *284*(2), 499-505.
- (29) Wehmeyer, K.R.; Wightman, R.M. *J. Electroanal. Chem.* **1985**, *196*, 417.
- (30) Dinan, T. E.; Matlosz, M.; Landolt, D. *J. Electrochem. Soc.* **1991**, *138*(10), 2947.
- (31) Yap, W. T.; Doane, L. M. *Anal. Chem.* **1982**, *54*, 1437.

---

Table I. Electroactive Surface Area Data<sup>a</sup> For Microhole Array Electrodes in Aqueous and Nonaqueous Solutions.

<u>Electrode Type</u>	<u>Sovent</u>	<u>Initial</u>	<u>After 5 Hours</u>
Gold/Anopore	DMSO	1.3	1.3
Gold/Anopore	Water	0.7	5
Gold/Silane/Anopore	Water	1	2.2

---

<sup>a</sup>Areas expressed as the ratios of the experimental area to the ideal (see text) area.

## FIGURE CAPTIONS

Figure 1. Background cyclic voltammograms at  $100 \text{ mV s}^{-1}$  at a microhole array electrode (solid) and a gold macroelectrode (dashed) in  $0.2 \text{ M LiClO}_4 / \text{DMSO}$ . The geometric area of both electrodes was  $0.33 \text{ cm}^2$ .

Figure 2. A. Cyclic voltammograms at the microhole array electrode for  $1.60 \text{ mM}$  ferrocene in  $0.2 \text{ M LiClO}_4 / \text{DMSO}$  solution. Scan rate  $= 50 \text{ mV s}^{-1}$ . Solution was quiescent (smooth) and stirred (spiked). B. Cyclic voltammograms demonstrating the transition from semi-infinite to finite diffusion in stirred solution. Scan rates were  $5, 20, \text{ and } 50 \text{ mV s}^{-1}$ ; geometric area of the electrode  $= 0.64 \text{ cm}^2$ .

Figure 3. Maximum current vs. square root of scan rate for voltammograms obtained at microhole array electrodes in quiescent ( $\circ$ ) and stirred ( $\bullet$ ) solutions. Solution was  $4.745 \text{ mM}$  in  $[\text{Fe}(\text{CN})_6]^{3-}$  aqueous  $1 \text{ M KCl}$ .



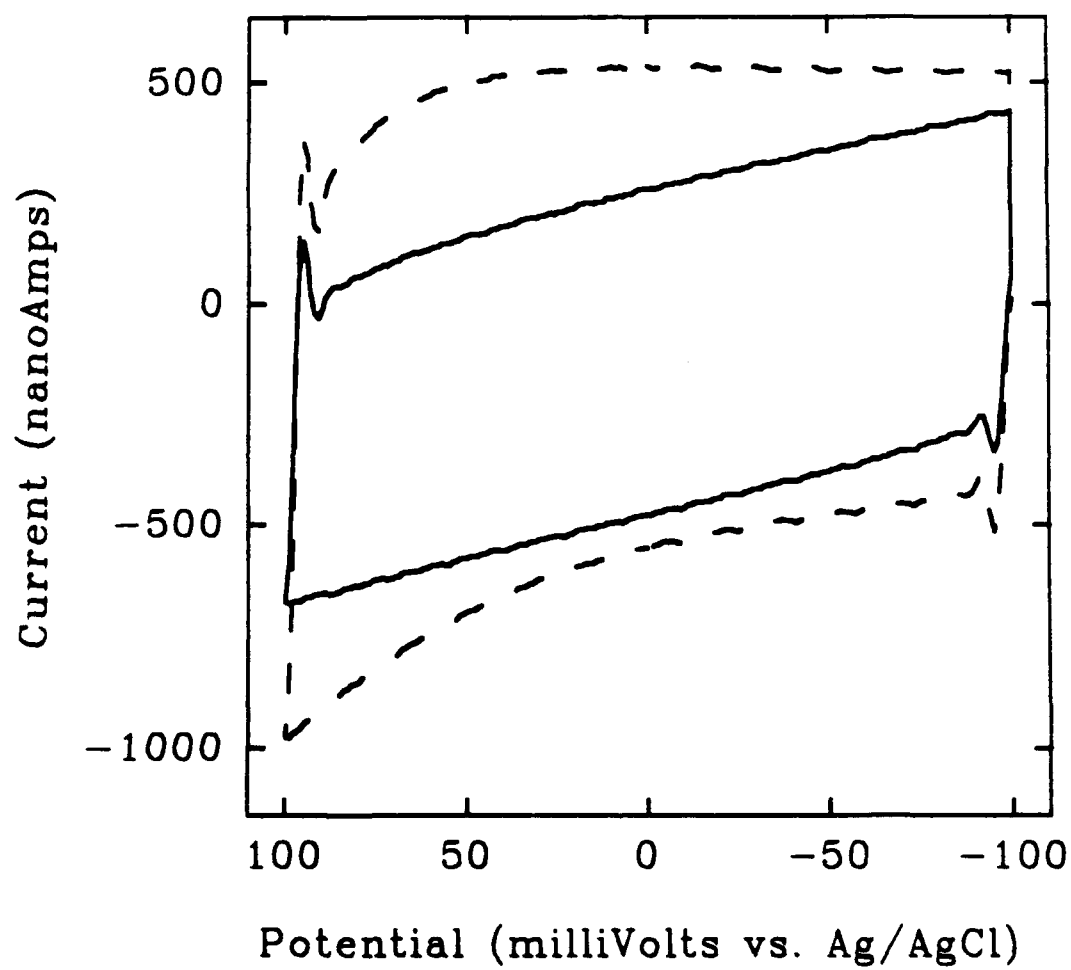
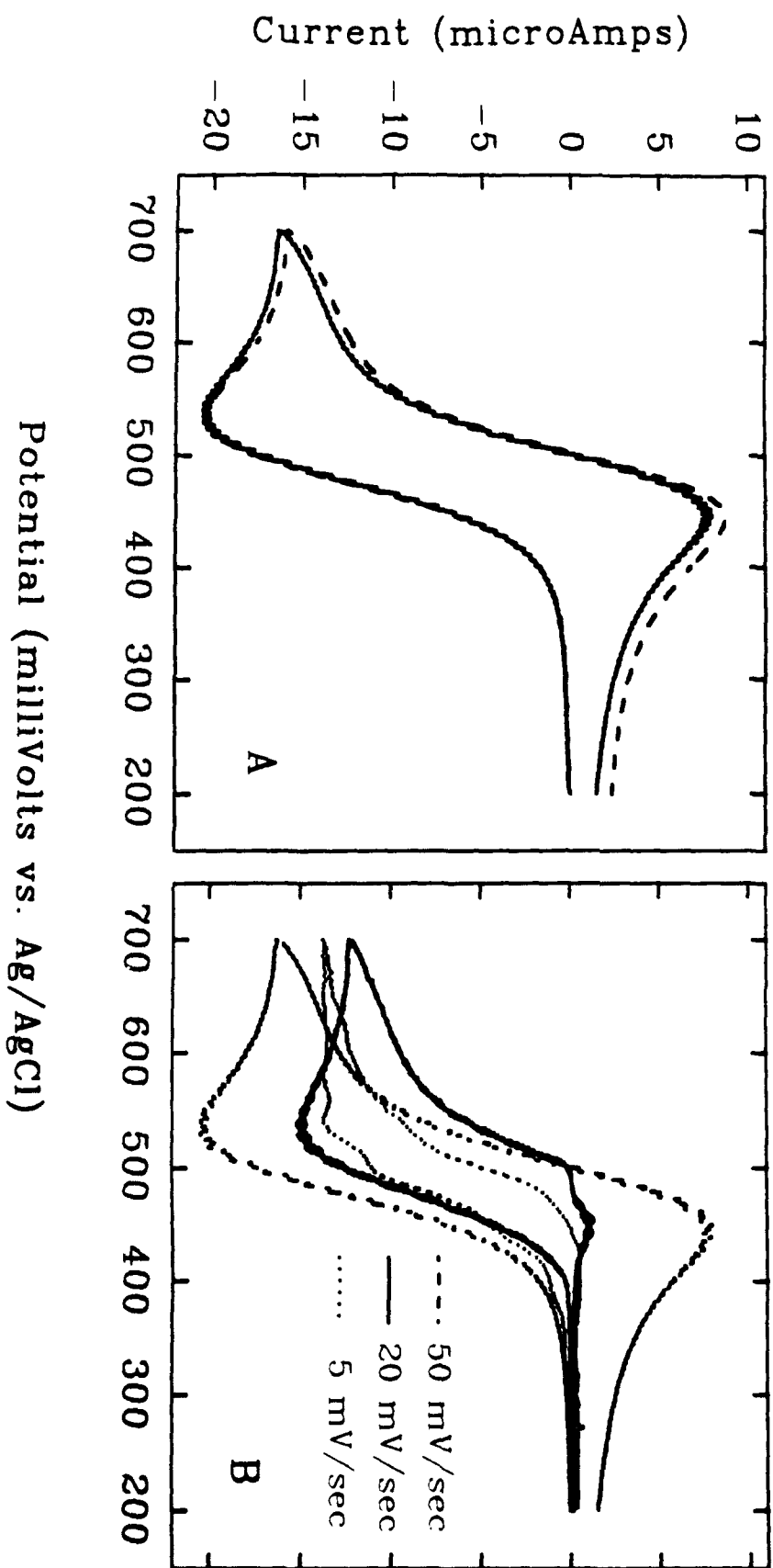


Fig 1



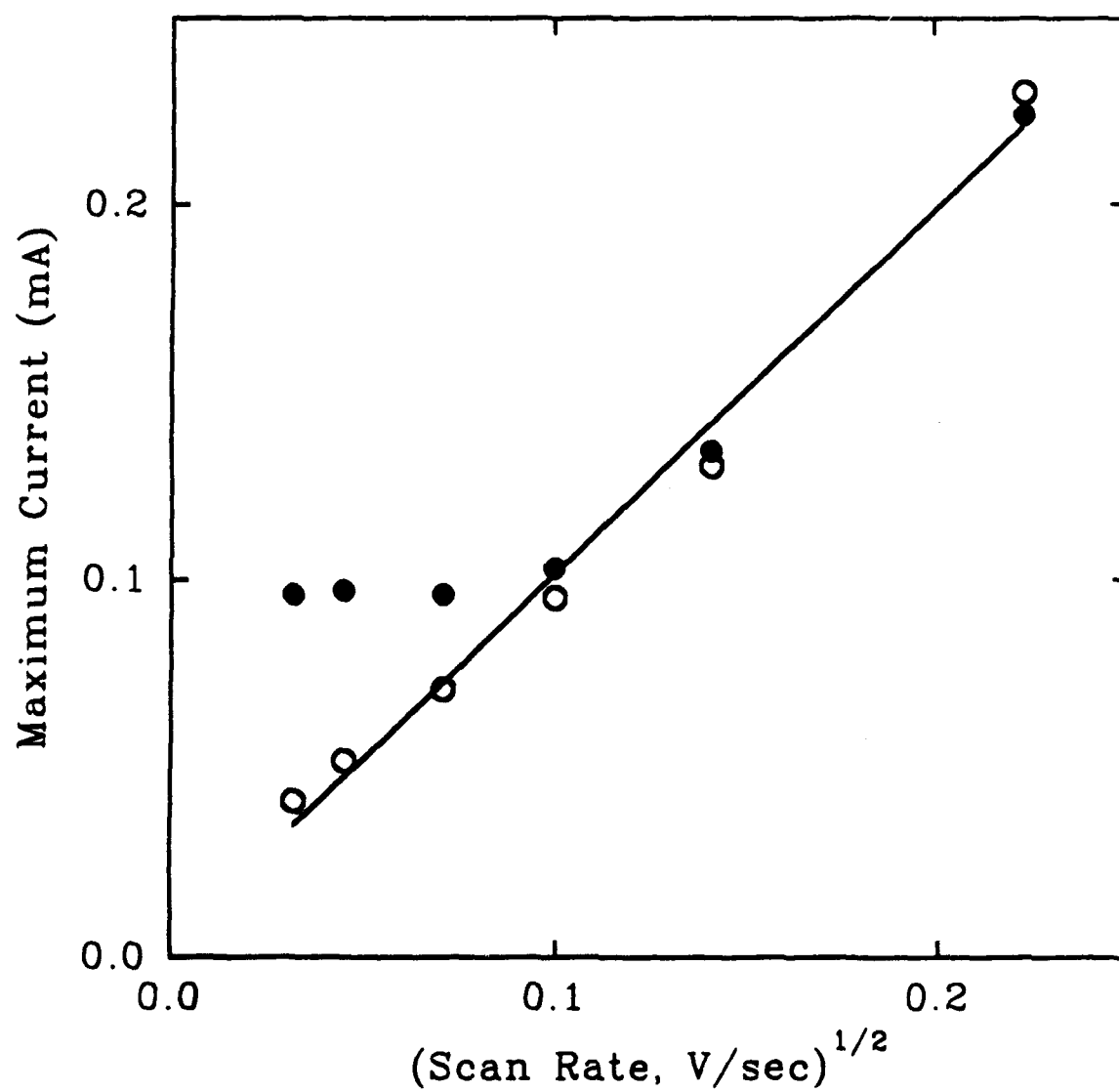


Fig 3